Electronic Supplementary Information

for

Thermal Deposition Method for p–n Patterning of Carbon Nanotube Sheets for Planar-type Thermoelectric Generator

*Ryohei Yamaguchi, Taiki Ishii, Masamichi Matsumoto, Angana Borah, Naoki Tanaka, Kaito Oda, Motohiro Tomita, Takanobu Watanabe, and Tsuyohiko Fujigaya**

Corresponding Author

Tsuyohiko Fujigaya: fujigaya.tsuyohiko.948@m.kyushu-u.ac.jp

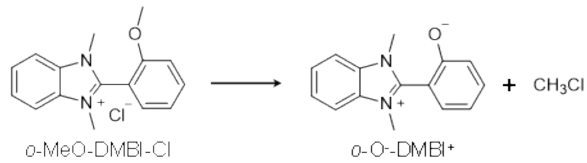

Scheme S1. Formation of *o*-O$^-$-DMBI$^+$ via thermal deposition of *o*-MeO-DMBI-Cl.

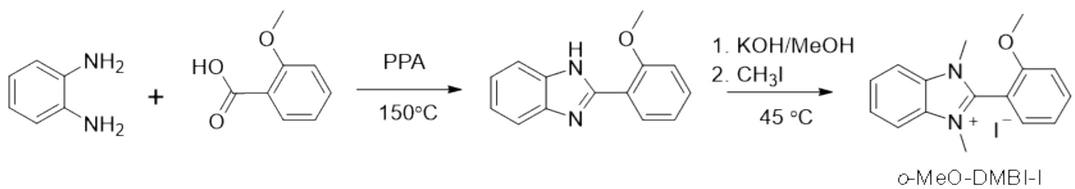

Scheme S2. Synthetic process to form *o*-MeO-DMBI-I.

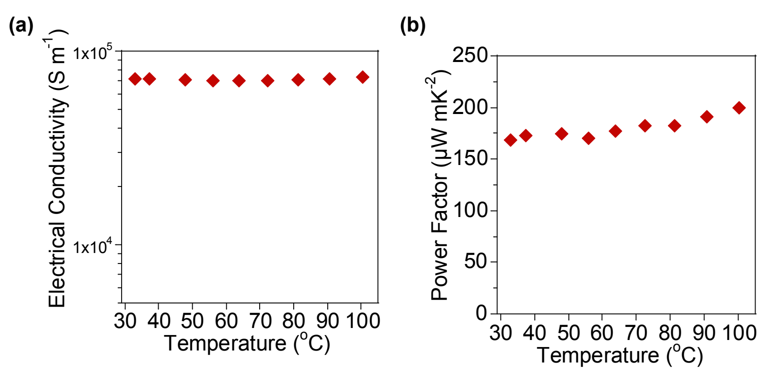

Fig. S1 Temperature dependence of the (a) electrical conductivity and (b) power factor of the deposited SWCNT sheets after post heating.

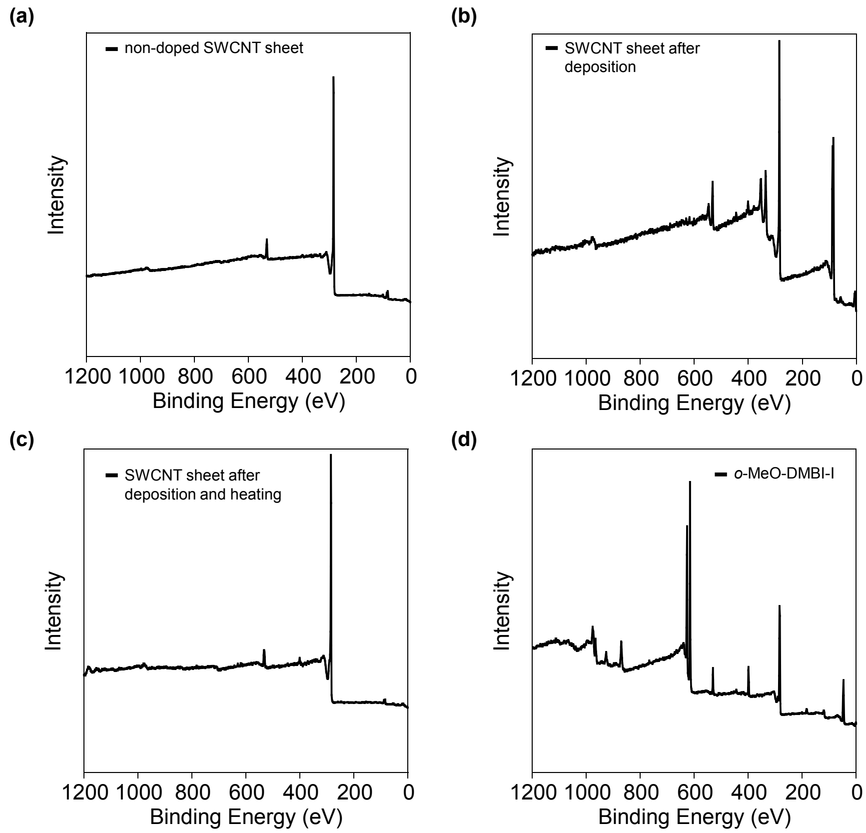

Fig. S2 X-ray photoelectron spectroscopy (XPS) survey scans of (a) non-doped single-walled carbon nanotube (SWCNT) sheet, (b) SWCNT sheet after deposition, (c) SWCNT sheet after deposition and post heating, and (d) 2-(2-methoxyphenyl)-1,3-dimethyl-1*H*-benzoimidazol-3-ium iodide (*o*-MeO-DMBI-I).

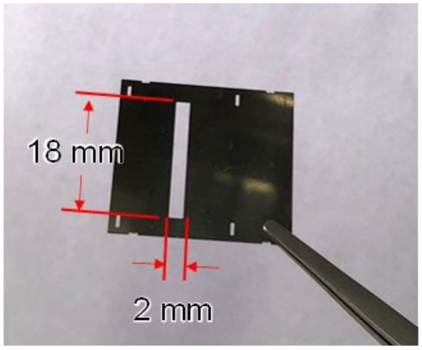

Fig. S3 Photograph of the mask.

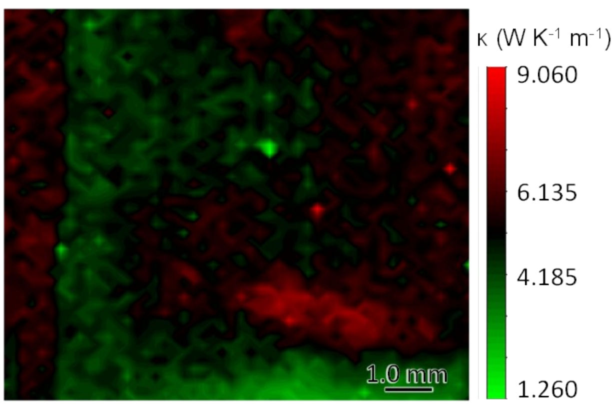

Fig. S4 Thermal conductivity mapping of the patterned single-walled carbon nanotube (SWCNT) sheet.

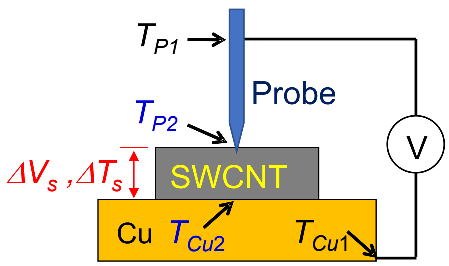

Fig. S5 Illustration of the scanning thermal probe microimaging. In this measurement, temperature of the probe (Constantan) top (T_{P1}) and substrate (Cu) bottom (T_{Cu1}) were measured, and the temperature of probe tip (T_{P2}) and substrate top (T_{Cu2}) were estimated based on Fourier Low, where the temperature difference between the top and bottom of SWCNT sheets (ΔT_s) was assumed as $\Delta T_s = T_{P2} - T_{Cu2}$. On the other hand, potential difference between the top and bottom of SWCNT sheets (ΔV_s) was estimated by subtracting potential gaps inside the probe and Cu from the measurement potential difference (V). Thus,

$$\Delta V_s = V - S_{constantan}(T_{P1} - T_{P2}) - S_{Cu}\,(T_{Cu1} - T_{Cu2})$$

where $S_{constantan}$ and S_{Cu} are Seebeck coefficient of constantan (–38.3 μV K^{-1}) and cupper (+1.9 μV K^{-1}), respectively.

And the S was determined as $S = \Delta V_s / \Delta T_s$ and was plotted in the 2D maps.

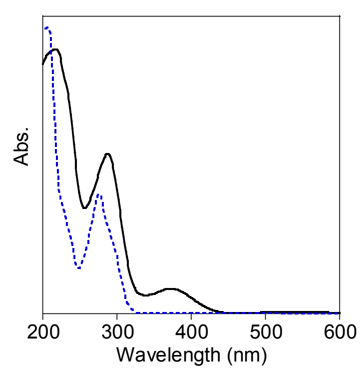

Fig. S6 (a) UV-vis-NIR spectrum of *o*-MeO-DMBI-I deposited on quartz substrate (black). The spectrum of *o*-MeO-DMBI-I in ethanol is also shown (blue).

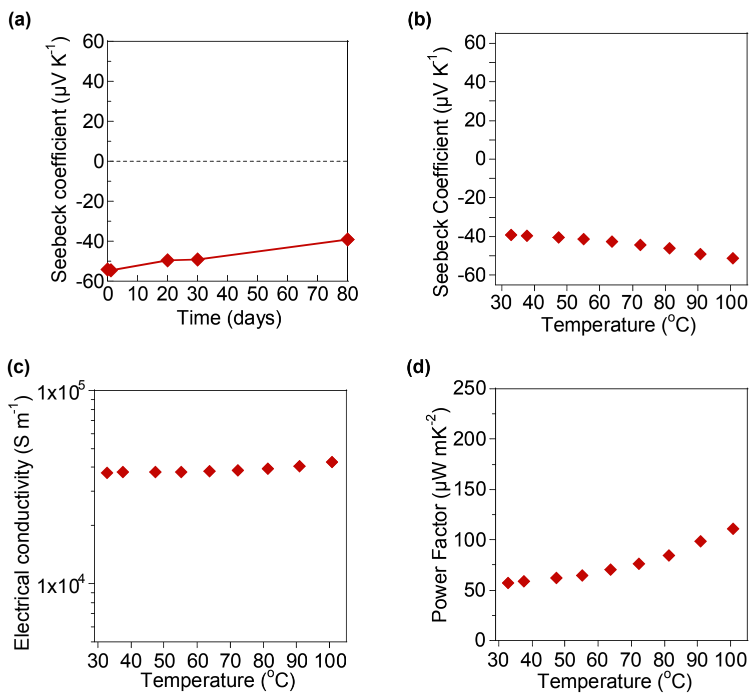

Fig. S7 (a) Air stability of the doped SWCNT sheet under atmospheric condition. Temperature dependence of the (b) Seebeck coefficient, (c) electrical conductivity and (d) power factor of the doped SWCNT sheets aged under atmospheric condition for 80 days.

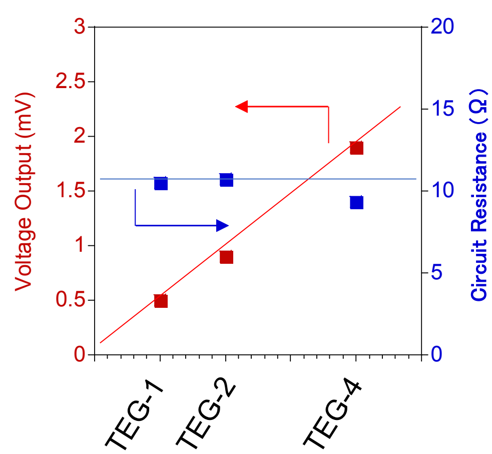

Fig. S8 Plot of open circuit voltage (OCV) (red) and circuit resistance (blue) for thermoelectric generators (TEGs) TEG-1, TEG-2, and TEG-4.

Table S1. List of power density per unit normalized by temperature difference for single-walled carbon nanotube (SWCNT)-based thermoelectric generators (TEGs).

n-dopant	Doping method	Year	P_{max} [nW]	OCV [mV]	ΔT [K]	Resistance [Ω]	ϕ (μWm^{-2}K^{-2})	Units	ϕ per unit (μWm^{-2}K^{-2} unit^{-1})	Device structure	Ref.
PVDF	solution mix	2012	137	26	50	1270	0.019	36	0.000528	π-type	S1
Polystyrene	solution mix	2013	5500	25.4	70	29.5	11.22	1985	0.005652	Unileg	S2
PEI:DETA	solution mix	2014	1800	300	32	11500	2.19	72	0.030417	π-type	S3
CPE-PyrBlm4	solution mix	2015	0.4	2	40	not provided	0.00259	4	0.000648	planar	S4
BMIM PF6	drop cast	2017	0.5	2.3	9	not provided	0.144	8	0.018	π-type	S5
NDINE	solution mix	2017	3300	22	50	not provided	1.1	5	0.22	π-type	S6
PEI	drop cast	2017	2500	11	27.5	12	20.74	3	6.91	π-type	S7
Oleamine	electron spray	2020	4640	45	44.4	47	35	15	2.3	π-type	S8
N-DMBI	solution dip	2020	1480	32	60	171	0.274	5	0.0548	π-type	S9
o-MeO-DMBI-I	thermal deposition	2020	96	1.9	25	9.3	0.96	4	0.24	Planar	This work

[a)]PVDF: polyvinylidene fluoride; [b)]PEI: polyethylenimine, DETA: diethylenetriamine; [c)]CPE-PyrBlm4: conjugated polyelectrolytes-pyridine Blm4; [e)]BMIMPF6: 1-butyl-3-methylimidazolium hexafluorophosphate; [f)]NDINE: naphthalene diimide; [g)]N-DMBI; 1,3-dimethyl-2-phenyl-2,3-dihydro-1*H*-benzimidazole; [h)]*o*-MeO-DMBI-I: 2-(2-methoxyphenyl)-1,3-dimethyl-1*H*-benzoimidazol-3-ium iodide.

References

S1. Hewitt, C. A.; Kaiser, A. B.; Roth, S.; Craps, M.; Czerw, R.; Carroll, D. L., Multilayered carbon nanotube/polymer composite based thermoelectric fabrics. *Nano Lett.* **2012,** *12*, 1307-1310.

S2. Suemori, K.; Hoshino, S.; Kamata, T., Flexible and lightweight thermoelectric generators composed of carbon nanotube–polystyrene composites printed on film substrate. *Appl. Phys. Lett.* **2013,** *103*, 153902.

S3. Kim, S. L.; Choi, K.; Tazebay, A.; Yu, C., Flexible Power Fabrics Made of Carbon Nanotubes for Harvesting Thermoelectricity. *ACS nano* **2014,** *8*, 2377-2386.

S4. Mai, C.-K.; Russ, B.; Fronk, S. L.; Hu, N.; Chan-Park, M. B.; Urban, J. J.; Segalman, R. A.; Chabinyc, M. L.; Bazan, G. C., Varying the ionic functionalities of conjugated polyelectrolytes leads to both p- and n-type carbon nanotube composites for flexible thermoelectrics. *Energy Environ. Sci* **2015,** *8*, 2341-2346.

S5. Ito, M.; Koizumi, T.; Kojima, H.; Saito, T.; Nakamura, M., From materials to device design of a thermoelectric fabric for wearable energy harvesters. *J. Mater. Chem. A* **2017,** *5*, 12068-12072.

S6. Wu, G.; Zhang, Z.-G.; Li, Y.; Gao, C.; Wang, X.; Chen, G., Exploring High-Performance n-Type Thermoelectric Composites Using Amino-Substituted Rylene Dimides and Carbon Nanotubes. *ACS Nano* **2017,** *11*, 5746-5752.

S7. Zhou, W.; Fan, Q.; Zhang, Q.; Cai, L.; Li, K.; Gu, X.; Yang, F.; Zhang, N.; Wang, Y.; Liu, H.; Zhou, W.; Xie, S., High-performance and compact-designed flexible thermoelectric modules enabled by a reticulate carbon nanotube architecture. *Nat. Commun.* **2017,** *8*, 14886.

S8. Sun, T.; Zhou, B.; Zheng, Q.; Wang, L.; Jiang, W.; Snyder, G. J., Stretchable fabric generates electric power from woven thermoelectric fibers. *Nat. Commun.* **2020,** *11*, 1-10.

S9. Hu, Q.; Lu, Z.; Wang, Y.; Wang, J.; Wang, H.; Wu, Z.; Lu, G.; Zhang, H.-L.; Yu, C., Double doping approach for unusually stable and large n-type thermoelectric voltage from p-type multi-walled carbon nanotube mats. *J. Mater. Chem. A* **2020,** *8*, 13095-13105.